Proceedings of The Institute of Acoustics

WITHIN-PULSE DOPPLER SCANNING USING FREQUENCY-DOMAIN PROCESSING

R.J. Heald and D.J Creasey

Department of Electronic and Electrical Engineering,
The University of Birmingham, Birmingham B15 2TT, England.

INTRODUCTION

In the time-domain, a target with a radially closing velocity will compress a reflected waveform, whilst a target with a negative radial velocity will stretch a reflected waveform. The amount by which a waveform is stretched or compressed depends upon the relative radial velocity of the target compared to the velocity of propagation in the supporting medium. A measure of the Doppler expansion or compression is the Doppler compression factor, a, defined as;

$$a = (c - v)/(c + v) \quad (1)$$

If a waveform undergoes a Doppler compression a, the resulting waveform will be identical to the starting waveform but all occurrences of the variable t in the defining equation are replaced by t/a. The waveform duration is changed from say t_1 to $a.t_1$. A Doppler shift may be described mathematically as,

$$f(t) \text{ ----Doppler Shift----> } f(t/a) \quad (2)$$

where f( ) is an arbitrary function.

In the frequency-domain the effect of a Doppler shift is of a reciprocal nature relative to the same effect viewed in the time-domain. If F(w) is the spectrum of a signal, then after a Doppler shift this spectrum becomes a.F(a.w). The mapping equivalent to (2) is

$$F(w) \text{ ----Doppler Shift----> } a.F(a.w) \quad (3)$$

Comparing (2) and (3) shows that if a Doppler compression occurs in the time-domain, (a<1), this creates an expansion in the frequency domain together with a scaling factor.

ECHO DETECTION VIA CORRELATION

In an echo-location system, optimum detection can be approximated by matched filtering [1]. A matched filter has a frequency-domain transfer characteristic which is the complex conjugate of the spectrum of the signal to which the filter is matched. Matched filtering can also be accomplished by correlation [2].

A practical scheme for the presentation of the processed information would be a plot or graph of 'Doppler-derived velocity' against 'range'. This can be achieved by a system of scanning in both range and velocity whilst making a comparison with a known signal. This scheme could be described as a point-by-point interrogation generating a probability output. Such a system produces a plot which is called an ambiguity diagram. In practical terms the interrogation process could be performed by correlation. Velocity and range scanning can be accomplished by compensating for the effects of the particular velocity and range being scanned prior to the correlation.

The Wiener-Kinchin theorem states that if $c_{xy}(T)$ is the cross-correlation function of two time functions x(t),y(t) and $C_{xy}(w)$ is the Fourier transform of

$c_{xy}(T)$, then

$$C_{xy}(w) = X(w).Y^{*}(w) \quad (4)$$

where X(w) and Y(w) are the Fourier transforms of the time functions x(t) and y(t). (The '*' denotes complex conjugate.) This theorem is utilised in the scheme being outlined. Equation (4) can be compared with the time-domain correlation equation

$$c_{xy}(T) = \int_{-\infty}^{\infty} x(t).y(t-T)\,dt \quad (5)$$

Equation (5) yields a single point indicative of the degree of correlation between the replica and the received signal with a lag T. However, in the frequency-domain, correlation is merely the product of one spectrum with the complex conjugate of another. This generates a third spectrum referred to as a cross-spectrum. Using the inverse Fourier transform of $C_{xy}(w)$ results in a number of correlation coefficients which are associated with a number of range cells. In practice, some form of the discrete Fourier transform (DFT) is often used and the discrete equation equivalent to equation (4) is a circular correlation. Suppose the duration of the transmitted signal is $N_1.\Delta t$ and the processed time window is $N.\Delta t$, where $1/\Delta t$ is the sampling frequency. Then the number of meaningful correlation coefficients is $(N-N_1)$ spaced Δt apart along the lag axis. Multiple correlation samples are obtained because of the scanning action created by equation (4). The missing N_1 points are lost because of the circular process introduced by using the DFT and finite time windows. Scanning in the range dimension is achieved by the frequency-domain process automatically. If the size of the scanned range needs to be increased either N is made larger or the process is replicated for another time window of size $N.\Delta t$.

REDUCTION OF PROCESSING OVERHEADS

Consider the processing overheads induced by working in the time-domain. The cross-correlation of two similar signals with non-zero centre frequencies, results in a cross-correlation envelope superimposed upon a centre-frequency component. Since it is the envelope which is of interest the centre-frequency component needs to be removed. This can be accomplished using quadrature channels and hence a two-channel correlation process. The results from these two channels are square and added together to form an output free of the centre frequency component. If a base-banded signal is used in the correlation the number of required channels is doubled. Let the number of samples used to construct a base-banded replica of the transmitted signal be N_1. The number of operations required to generate one correlation function sample is $(4.N_1+2)$.

To generate a range velocity ambiguity diagram, both range and velocity need to be scanned, this can be done by a scheme of compensation. Range compensation and hence scanning can be accomplished by sliding the echo time window along the time axis. Velocity compensation amounts to applying an appropriate Doppler distortion. If there are to be M range cells and P velocity cells, then this process requires M_1 operations to generate the required plot, where M_1 is given by

$$M_1 = 2.P.M.(2.N_1+1) \quad (6)$$

Here an operation is of the form A=B.C+D where all the operands are real.

Consider working in the frequency-domain. Using baseband signals the data points are fed into the Fourier transform as complex numbers. The process generates $(N-N_1)$ cross spectral coefficients. Thus to generate an M range-cell against P velocity-cell plot, the number of operations required is

$$M_2 = 2.P.M.\{(FT)_m+3.N\}/(N-N_1) \quad (7)$$

where $(FT)_m$ is the number of operations required to perform a Fourier transform.

If the length of Fourier transform is N and the radix-2 fast Fourier transform (FFT) is used then the number of operations required to realise each Fourier transform is given by

$$(FT)_m = 2.N.\log_2(N) \quad (8)$$

Thus the total number of operations required to generate the range against velocity plot in the frequency-domain is

$$M_2 = P.M.N.\{6+4.\log_2(N)\}/(N-N_1) \quad (9)$$

Note that the FFT is not necessarily the best algorithm for this purpose but is used here to demonstrate the principle. It has also been assumed that samples of the replica spectra are available.

If we calculate the ratio of the number of required operations in the time-domain to the number required in the frequency-domain then the result (MR. - Multiplications Ratio) will given an indication of the relative levels of processing overheads. The accuracy of this indicator is dependent upon the hardware used to impliment the calculation scheme. From equations (6) and (9)

$$MR. = \frac{(2.N_1+1).(N-N_1)}{N.\{3+2.\log_2(N)\}} \quad (10)$$

From equation (10) if N_1=200 then values of N above 221 result in a more favourable processing overhead if working in the frequency-domain.

VELOCITY SCANNING

To generate an ambiguity diagram, the value of the correlation function needs to be evaluated for all range and velocity cells within the diagram. That is, if there are M range cells and P velocity cells, then the correlation function, c(r,v) needs to be evaluated for r=1 to M and for v=1 to P. Velocity scanning can be accomplished by using multiple replicas, each with a different Doppler distortion. This is computationally burdensome because of the replication of storage and the number of data transfers required. A more efficient scheme of velocity scanning could be implemented by taking a single replica and producing from this the necessary Doppler shifted replicas. A scheme has already been employed [3] when considering velocity scanning in the time-domain. The reciprocal nature of the Doppler effect in the time and frequency-domains predicts a similar scheme in the frequency-domain.

NON-UNIFORM SHIFT REGISTER

A non-uniform shift-register (NUSR) structure can be used to perform velocity

scanning. The design requirement of the structure is that given one set of samples of any replica signal, a simple repetitive action will generate incremental Doppler-shifted versions without the need for multiple replica storage. If this repetitive action is assumed to be a serial data shift, the scheme outlined would require P serial data shifts to generate P different Doppler distorted versions of the replica signal. Hence velocity scanning is performed.

Consider the Doppler effect in the time-domain. If samples of a signal are considered, Doppler compression can be produced by changing the sampling rate. Let a signal of duration T be sampled at a rate s. The number of samples required to store this signal is sT. If the sample rate is changed to as, the signal of duration T would require asT samples. If this second set of samples is interpreted as if the sample rate was still s, the apparent signal duration would be aT. This effect is the same as that generated by a Doppler compression.

If a_d is the Doppler compression factor associated with a relative radial velocity v_d, the following approximation can be used

$$a_d \simeq g^d \qquad (11)$$

where d is the velocity cell number, and integer, and g is a constant. The value of g is dictated by the maximum target speed and the number of velocity cells. The significance of the approximation of a_d by equation (11), is that to increment the Doppler shift applied to a signal, the sample rate is multiplied by g. This action becomes very simple if a geometric structure is used as illustrated in Fig.1. Let the input inter-sample separations follow the geometric series

$$k,\ k.g,\ k.g^2,\ k.g^3,\ k.g^4,\ k.g^5 \qquad (12)$$

see Fig.2. Here k is a constant. The output inter-sample separations then follow the same geometric series. Next, shift the data within the register in the direction indicated. The output inter-sample separations then follow the geometric series

$$k.g,\ k.g^2,\ k.g^3,\ k.g^4,\ k.g^5 \qquad (13)$$

As can be seen by comparing the sequences in (12) and (13) the inter-sample separations have been multiplied by g as a result of a single shift of the data. If d shifts are used, the inter-sample separations are multiplied by g^d as required for the d^{th} velocity cell.

As described the register is uniform. Non-uniformity is introduced by only using specific output taps. The location of these taps is described by a mapping which is inverse to the input inter-sample separations. The used output tap numbers are given by i where

$$i\text{-}n_2 = (\log_2\{1+[n_3\text{-}h].[1\text{-}g]/g\})/\log_2 g \qquad (14)$$

The terms n_2 and n_3 are the total numbers of taps used at the input and output respectively (see Fig.3), where h is the output sample number which goes from 1 to n_3 in unit steps. The non-uniform sample positions of the input data are required to enable a serial data shift to create the appropriate data compres-

sion factor. The inverse non-uniformity, as depicted in equation (14) is required so that the resulting sequence appears as a set of uniformly positioned samples of the compressed replica. Fig.3 shows a block diagram of a system which takes as its input n_1 uniformly spaced samples with separation L. The matched reciprocal register, MRR, distorts these sample positions by tap selection to produce the required inter-sample positions as given by the sequence (12). The equation relating the MRR output sample numbers, j, to i, the NUSR inputs, is

$$(j-k).(g-1) = k.(g^{i-1}-1) \qquad (15)$$

The final n_3 output samples are uniformly spaced z_d apart with the value of z_d set by d serial shifts in the NUSR. Such a system has the potential of being able to produce Doppler-shifted spectra which act as multiple replicas for any chosen signal whose samples are inputted into the NUSR.

RESULTS OF SIMULATION

The system discussed was simulated in Fortran on a Honeywell Multics computer. The presentation of results takes the form of a three-dimensional projection. The signal processing scheme is independent of the type of signal used and for purposes of simulation a number of different typical signal types have been investigated. Typical system outputs are shown in Fig.4 and Fig.5.

REFERENCES

[1] A.W. Rihaczek, "Principles of high resolution radar", McGraw-Hill.

[2] D.O. North, "An analysis of the factors which determine signal/noise discrimination in pulsed-carrier systems", Proc.IEEE, Vol. 51, no.7, 1015-1027, June 1963.

[3] M.H. Yassaie, D.J. Creasey, "Doppler scanning correlator", IEE. Conference Digest 1985/47.

WITHIN-PULSE DOPPLER SCANNING USING FREQUENCY-DOMAIN PROCESSING

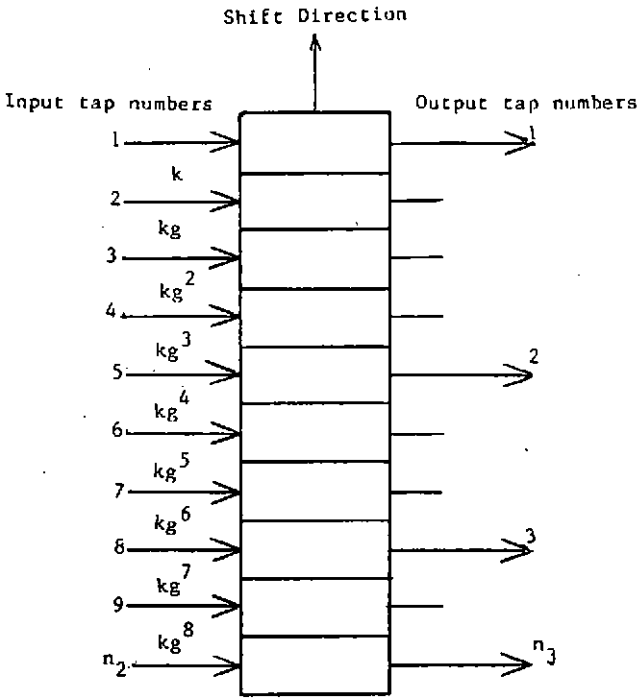

Fig.1 NUSR Structure

NUSR Input Sampling Scheme

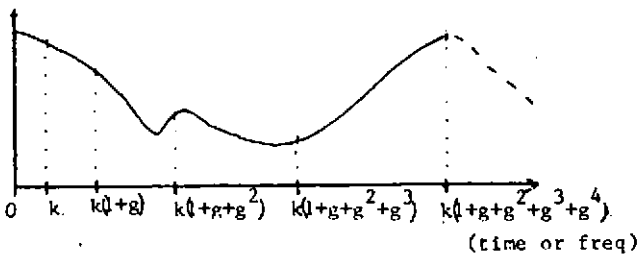

Fig.2 Sampling Positions

WITHIN-PULSE DOPPLER SCANNING USING FREQUENCY-DOMAIN PROCESSING

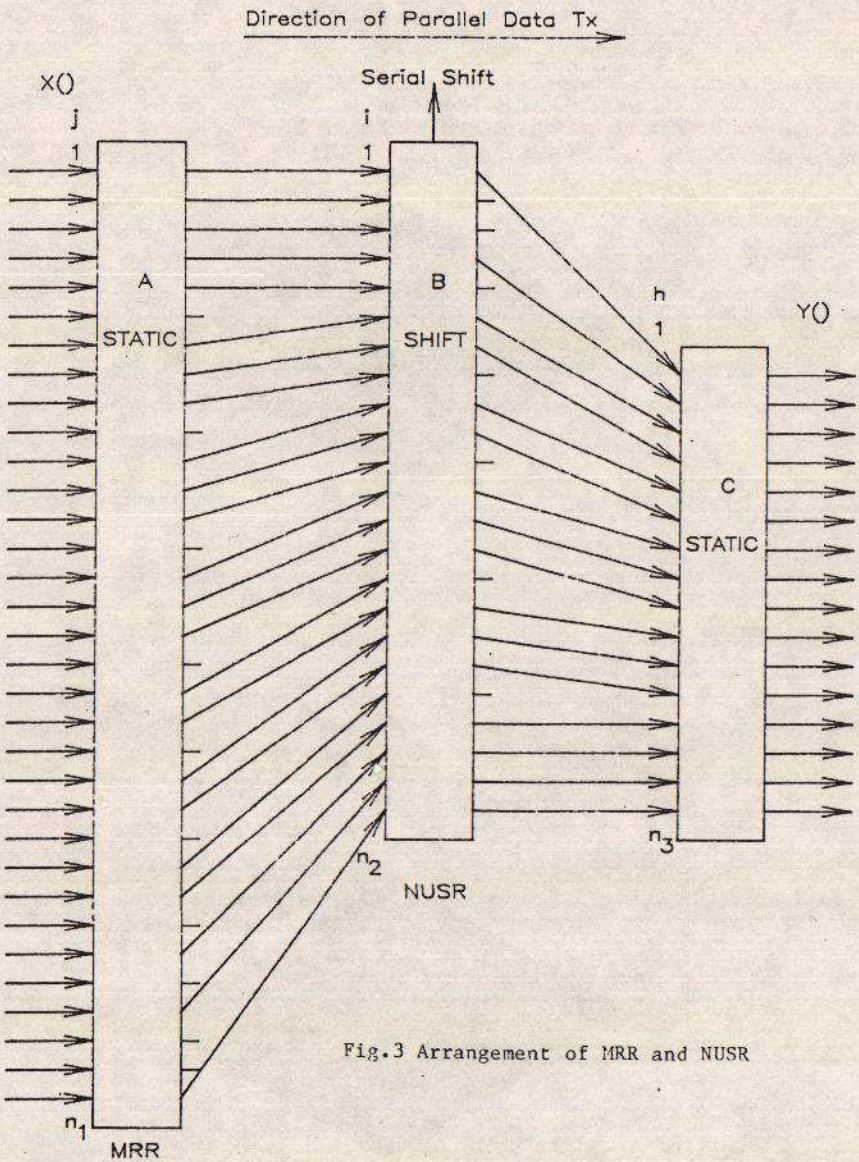

Fig.3 Arrangement of MRR and NUSR

WITHIN-PULSE DOPPLER SCANNING USING FREQUENCY-DOMAIN PROCESSING

TRANSMITTED SIGNAL	
Linear "UP" Chirp	
Bandwidth time product	16
Pules length (ms)	11
Bandwidth (Hz)	1440
Chirp centre frequency (Hz)	11520
Number of samples in Echo	512

TARGET POSITION	
Range	Velocity
25.00	0.00
35.00	−50.00

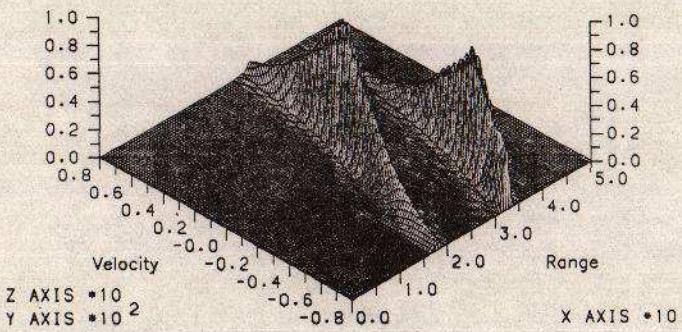

Fig (4)

TRANSMITTED SIGNAL	
Linear "UP − VEE" Chirp	
Bandwidth time product	16
Pules length (ms)	11
Bandwidth (Hz)	1440
Chirp centre frequency (Hz)	11520
Number of samples in Echo	512

TARGET POSITION	
Range	Velocity
25.00	−10.00
35.00	−50.00

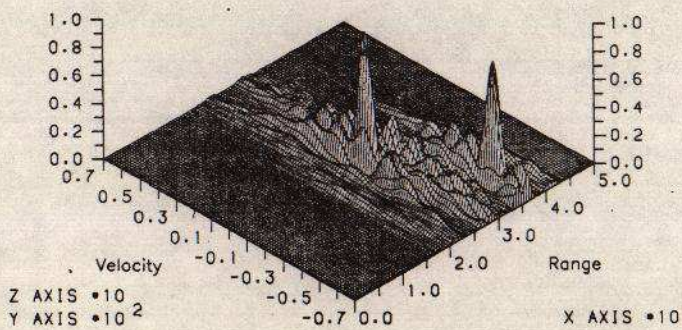

Fig (5)

Proceedings of The Institute of Acoustics

A WIDE BAND CONSTANT BEAM WIDTH ECHO SOUNDER FOR FISH ABUNDANCE ESTIMATION

E. J. Simmonds and P. J. Copland
Marine Laboratory, Victoria Road, Torry, Aberdeen

INTRODUCTION

To estimate the abundance of pelagic fish acoustically Echo Integration can provide a measure of biomass, or the number of fish. This method assumes that the average fish backscattering strength or target strength (TS) is predictable. Present procedures require that the TS does not depend significantly upon fish behaviour, and that echoes from species of interest can be easily distinguished from those of less importance. The identification is usually done either by visual inspection of echo traces or by partition of the echo integrator data in proportion to the composition of trawl catches. The target strength is usually assumed to be constant, or perhaps dependent on fish length but independent of fish behaviour. Unfortunately, this is probably too simple a model. Fish are known to have highly variable back scattering strengths which depend upon tilt angle [1, 2]. Moreover the size of the gas-filled swimbladder will change with the depth of the fish [3, 4]. At normal survey echo sounder frequencies the acoustic wavelength is generally of the same order as some of the dimensions of the fish. It is therefore expected that there will be some frequency dependance in back scattering strength resulting from both changes in tilt angle and swimbladder size.

By increasing the system bandwidth it might be possible to use frequency response information to help identify species or swimbladder size, or to smooth out differences in back scattering strength due to fish orientation changes. A wide band echo sounder has been produced to investigate these possibilities.

The main feature of a wide band system is that the transducer beam shape both on transmission and reception should remain relatively constant and independent of frequency, thus ensuring that the sample volume is not frequency dependent. In addition there is a need to keep the sample volume size similar to that used in present surveys so that data collected from such a system can be used directly with our present knowledge of fish reflectivity. Thus a wide band system opperating around about the most commonly used frequency of 38 khz is desirable. Several approaches have been suggested and tried over the years using nonlinear acoustics for transmission and or reception and twisted arrays for reception [5, 6] .

The technique chosen [7] uses a partial sphere transducer which provides constant beam width transmission and reception in a single unit. The transducer is constructed from elements arranged in concentric rings on the surface of a partial sphere. These rings are amplitude shaded on transmission and reception to form the required beam shape. The system has been designed with a multifrequency transmitter and multichannel variable gain receiver. The equipment is described in this paper along with the results from an initial series of experiments on acclimatised and preacclimatised cod, and on herring.

EQUIPMENT

Wide Band Echo Sounder

The transducer (Figure 1) is constructed from 217 elements arranged in eight concentric rings surrounding a central element, on the surface of a partial sphere. The individual

transducer elements are of a pre-stressed sandwich resonator type with 20 mm diameter aluminum head and 10 mm steel tail mass. The case is machined from a solid cast block of nylatron GSM. The active face of the transducer subtends an angle of 28.3° and has a radius of curvature of 86cm, giving a nominal beam width of 10.5°. The casing is left proud at the edges to protect the face, and an underwater housing containing transmit and receive shading components is situated on the back of the transducer. The constant beam width is formed using frequency independent amplitude shading on both transmit and receive. This shading functions for transmit and receive are the same. They are shown in figure 2. On transmit, the voltage shading is produced from an autotransformer with nine taps, one for each ring of the transducer. On receive the same shading function, which depends upon the number of elements and is therefore different from ring to ring, is implemented using a single low noise operational amplifier per ring with a summing point amplifer to form the beam. Both the receive and transmit shading components are contained in the housing on the back of the transducer, along with mercury loaded reed relays which are used for transmit-receive switching. The transducer thus has a single transmit drive, and a single receive line along with transmit-receive switching and receiver power supplies.

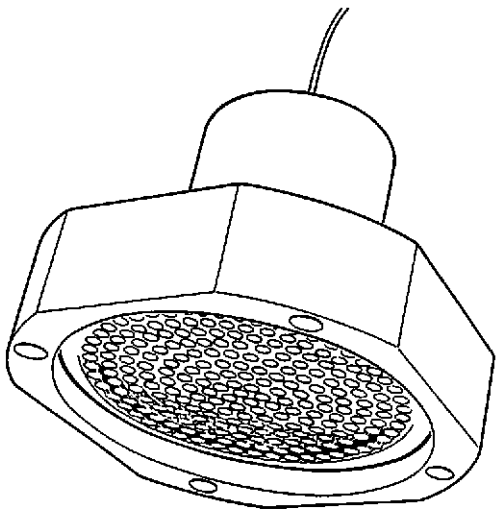

Figure 1 Transducer with 217 elements arranged on a partial sphere

The transmitter consists of a modulator providing ½, 1, 2, 4 and 8 millisecond pulses. For the present experiments a 1 ms pulse was used and, 32 digitally selected frequencies from 27 to 54kHz. The power stage is a 1kw mos-fet amplifier which operates up to 100kHz. The system is shown in Figure 2.

The receiver has a low noise operational amplifier stage for each ring housed in the back of the transducer and a summing point amplifier to provide the beam forming. This stage has a wide band filter and a 50ohm line driver to match the cable. The signal is then connected to eight frequency channels each with a five resonator filter giving 3.3kHz bandwidth between 3dB points, followed by two gain stages with computer control of gain to match the differences in transducer sensitivity with frequency. Each frequency channel has a separate detector, and the outputs are multiplexed and sampled at 100kHz with 12 bit binary precision giving a 12.5kHz sample rate per channel (80μs interval).

A WIDE BAND CONSTANT BEAM WIDTH ECHO SOUNDER

Figure 2 Wide Band System Block Diagram

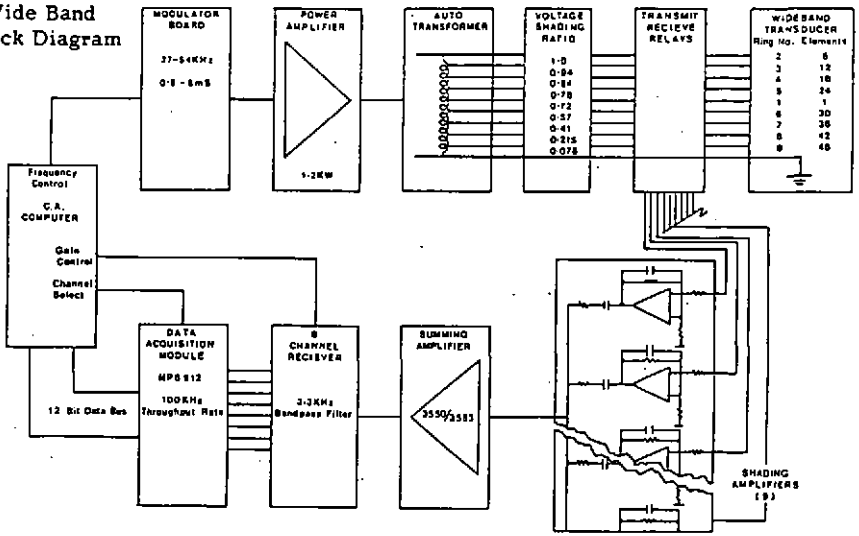

Experimental Rig

Measurements of the transducer beam shape and the spectoral response of fish were carried out at Marine Laboratorys, Loch Duich field station which is on the west coast of Scotland. Fish were placed in a cage 2m diameter and 1.5m deep (Figure 3). The cage was placed between two aluminium frames supporting stereo 35mm still cameras and low light TV cameras below the cage [8]. The complete rig was suspended from a raft, the transducer at 15m below the surface in a motorised gimbal table [9] with a 38.1 mm diameter tungsten carbide reference target positioned 10m further down. The cage support frame was 12m from the transducer which placed the fish at a range of 14m from the transducer. This arrangement allowed the ball to be used as a reference target, with transducer position adjusted for maximum echo strength and the fish located in the region of the centre of the beam. Photographs were taken throughout the experiments to provide a measure of the fish distribution and behaviour within the cage. Acoustic data were collected using the 32 transmit frequencies sequentially with a 300msec repetition rate. Results were collected into 1 hour blocks. The beam patterns were measured by removing the cage and camera frames and recording the echo from the reference target only. The transducer was steered through a range of angular locations using the motorised gimbal table. The method of obtaining the equivalent beam angle is described in [10].

RESULTS

Beam Angle Measurements

The measured beam angles are shown in Figure 4a. This has been replotted showing deviation from the theoretically predicted sample volume in 4b, and for the section of the beam which passes through the experimental fish cage (Figure 4)c.

Figure 3 Experimental rig (not to scale)

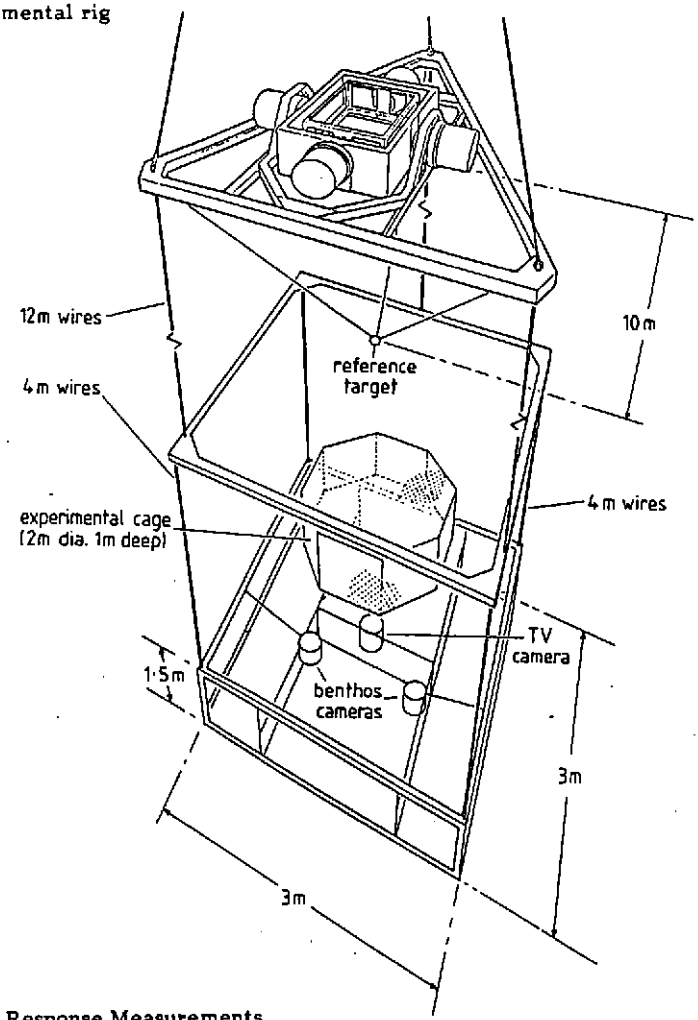

Fish Frequency Response Measurements

Four experiments were carried out, two with cod and two with herring. The number of fish and size ranges are shown in Table 1. For all experiments the fish were removed from a surface holding pen and placed in the experimental cage, lowered to a depth of 29 m and left for several days. During this period stereo photographs were taken every ½ hour and acoustic data collected in 6 minute blocks of 40 transmissions per frequency, over 32 fixed frequencies placed linearly between 27 and 54 kHz. The acoustic data were averaged over 1 hour periods before further analysis. Herring, once lowered to depth produce relatively consistant results over several days. These experiments ran for 3 days. The first hour of data was ignored. In the case of cod, the fish slowly adapted to the higher pressure and

produced stable results after 3 days. Clear differences occurred in the acoustic reflectivity between day and night. The data from the cod experiments were divided between four time categories: " day", from 0500 hours to 2100; "night", 2100 to 0500; "preacclimatised", less than 48 hours at experimental depth; and "acclimatised", more than 72 hours at experimental depth, the intervening 24 hour period was neglected. These criteria were selected purely on the basis of acoustic data, in particular the results of earlier single frequency work [11].

Figure 4 Equivalent Beam Angle

a) dB rel 1 steradian
b) dB rel theoretical model
c) within fish cage
dB rel 1 steradian

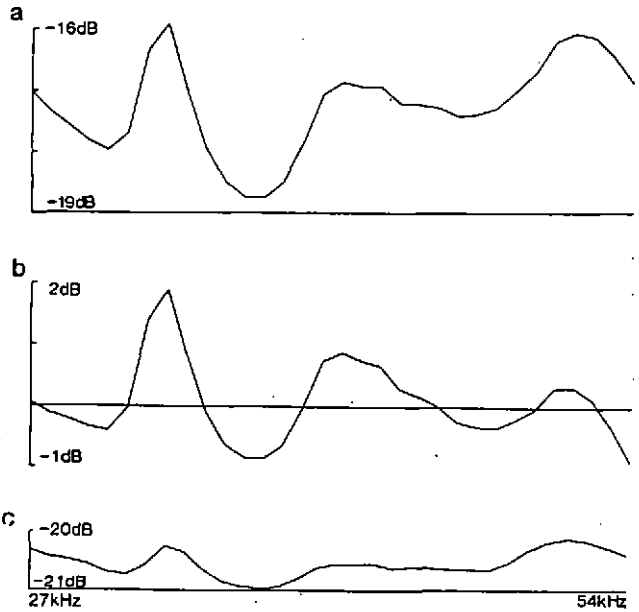

The performance of the acoustic system was monitored by a tungsten carbide reference target 10 m from the transducer. The calculated frequency response of the reference target is shown in Figure 5. This was taken into account when analysing the fish data. In addition the beam shape showed some change with frequency (Figure 4c). The correction for this is also included in the data analysis.

Figure 5 Calculated Frequency Response (dB) for 38.1 mm diameter Tungsten Carbide Sphere

In the case of both cod and herring, no statistically significant differences were found between experiments. The acoustic data from all expeirments with the same species were combined.

During the experiments stereo pair photographs were taken once every half hour on two 35mm Benthos cameras. The data from experiments with cod were analysed and some of the results have been included here for comparison with the acoustic data. The stereo photographs provided data on the spacial distribution of fish within the cage, and fish orientation. These parameters were obtained for the same four time categories mentioned above.

Figure 6 Frequency response of cod at 95% confidence levels for cases (dB//m^2 steradian kg^{-1})

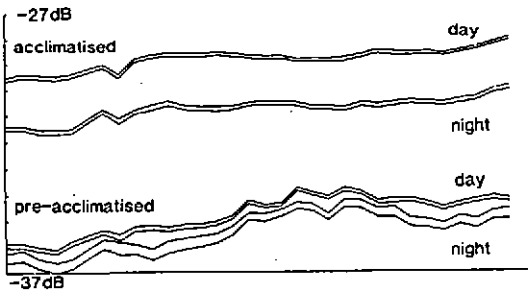

Figure 7 Relative frequency response (dB) for acclimatised and pre-asslimatised cod

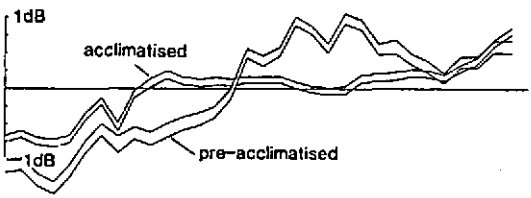

Figure 8 Relative frequency response (dB) for cod at night and during the day

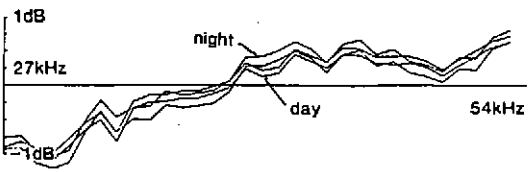

Figure 9 Relative frequency response (dB) for herring

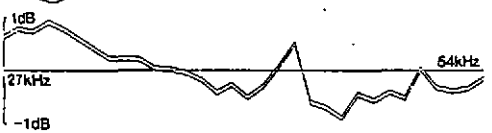

Figure 6a shows the acoustic backscattering strength per kilogram for cod with mean weight of 204g and mean length 27.0cm. This figure illustrates the absolute differences in backscattering strength between the four categories. Differences between mean values day and night are 2.0dB and 0.5dB for acclimatised and preacclimatised states respectively, and 5dB between the acclimatised and preacclimatised states. In addition there are other differences with frequency. Figures 7 and 8 show plots of relative frequency response for day and night data, and separately for acclimatised and preacclimatised fish. These show

no significant spectral difference between day and night, but there are statistically significant differences between acclimatised and preacclimatised fish. Figure 9 shows the relative response for herring, again showing significant differences from both acclimatised and preacclimatised cod.

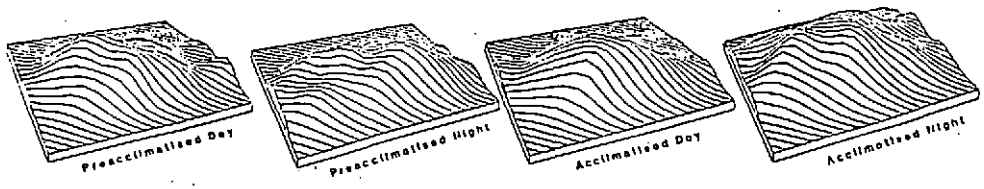

Figure 10 Horizontal distribution of cod within cage for 4 separate periods

Some results from the photographic data collected during experiments with cod are shown in Table 2 the mean tilt angle and mean interquartile range for the four categories these results are similar to those found before [12]. Figure 9 shows the horizontal distribution within the cages. The octagonal fish cage is located centrally in each plot of Figure 9, with four sides parallel to the edges of the plot. There are also differences in vertical distribution within the cage. However, this is compensated for directly by a digital TVG function.

Table 1

Experiment	$\bar{L}$ cm	$\bar{W}$ g	Number
1 Cod	26.8	200	35
2 Cod	27.2	208	36
1 Herring	27.4	172	66
2 Herring	26.5	177	46

Table 2
Tilt angles of cod

		Mean	Interquartile Range
Preacclimatised	Day	+ 5°	54°
	Night	+ 4°	44°
Acclimatised	Day	-11°	64°
	Night	-8°	59°

DISCUSSION

The acoustic results are significantly different between the four time categories of cod and for herring. Of particular interest is the clear change of slope between target strength functions for herring and for cod irrespective of acclimatisation state. If this can be shown to occur in free swimming fish, there are important implications for the separation of herring and gadoid species in the wild. For cod, two aspects of fish behaviour have been monitored which might explain some of the differences. A third physiological effect, that of the swim-bladder volume has not been investigated. However, it is assumed that the initial quadrupling of pressure would produce compression, followed in the case of cod by a slow secretion of gas to return the fish to neutral buoyancy, which it is expected would explain the 2 to 3 days of lower acoustic results. In the case of herring, no gas secretion takes place. The changes in radial distribution shown in Figure 9 show differences between night vs day and acclimatised vs preacclimatised states. The extremes are from acclimatised day periods when the fish are more concentrated in the centre of the cage, and preacclimatised night when the fish are most widely distributed. These small changes in distribution could give rise to some changes in absolute target strength and some smaller

changes in relative frequency response magnitude of such effects is uncertain, but it is expected that changes due to both factors would be to less than 0.5dB. Thus there are significant changes of greater than 4.5dB in absolute backscattering strength, and 1.5dB in the relative frequency response between acclimatised and preacclimatised fish. It is suggested that these amplitude effects are due to a combination of changes in both tilt angle and swimbladder volume, and that the changes in frequency response are primarily caused by changes in swimbladder volume.

CONCLUSIONS

The wide band system has considerable potential for the measurement of fish stocks. The system operates over an octave of frequency from 27 to 54kHz. The results from measurements on caged cod and herring indicate differences in frequency response which appear to be linked to swim-bladder volume, fish behaviour or both. Further work is required to determine the exact causes of such effects. However, the differences between cod and herring are important and may have useful applications

ACKNOWLEDGEMENTS

We would like to thank D N MacLennan for providing the frequency response of the tungsten carbide ball, S T Forbes for his assistance in developing the wide band system, and I B Petrie and T V Taylor for the assistance with the experimented work. In addition we would like to thank A.E. Magurran, T.J. Pitcher and C.E. Forster for their analysis of the stereo photographs.

REFERENCES

Nakken, O. and Olsen, K. 1978 Target strength measurements of fish, Hydro-Acoustics in Fisheries Research Bergen Symposium 1973. Edited A.R. Margetts. ICES Vol 170.

Foote, K. G. Rather-high-frequency sound scattering by swimbladdered fish JASAVd 79 No 2 pp 688-700 1985.

Sands O. and Hawkins A.D. Swimbladder volume and pressure in cod norm J. Zool. 22 31-34 1974.

Blaxter, J.H.S., Denton, E.J. and Gray, S.A.B. The herring swimbladder as a gas reservoir for the acoustics-lateralis system. J. Mar. Biol. Ass. 59 p 1-10. 1979.

Berktay, H.O., Dunn, J.R. and Grazey B.K. Constant beamwidth transducers for use in sonars with very wide frequency bandwidths. Applied acoustics 1 81-99 1968.

Berktay, H.O. and Learly D.J. For field performance of parametric transducers JASA Vol 55. No 3 pp 539-546. 1974.

Rodgers, P.H. and Van Buren, A.L. 1978 A new approach to constant beam width transducer. JASA 64(1), 38-43.

Edwards, J.I and Armstrong, F. 1983 Target strength measurements on herring sprat and mackerel 1983. ICES B:25. ICES CM1983/B:25.

Copland, P.J. 1984 A microprocessor based remote control and environmental monitoring system. Marine Laboratory Working Paper 1/84.

Simmonds, E.J. 1984 A comparison between measured and theoretical equivalent beam angles for seven similar transducers. J. Sound. Vib. 1984 97(1) 117-128.

Forbes, Simmonds and Edwards. Target strength of Gadoids. Bergen Symposium on Fisheries Acoustics June 1983.

Stewart, P.A.M. Prelliminary investigation of the tilt angle of caged fish. Marine Laboratory Working Paper 16/81.